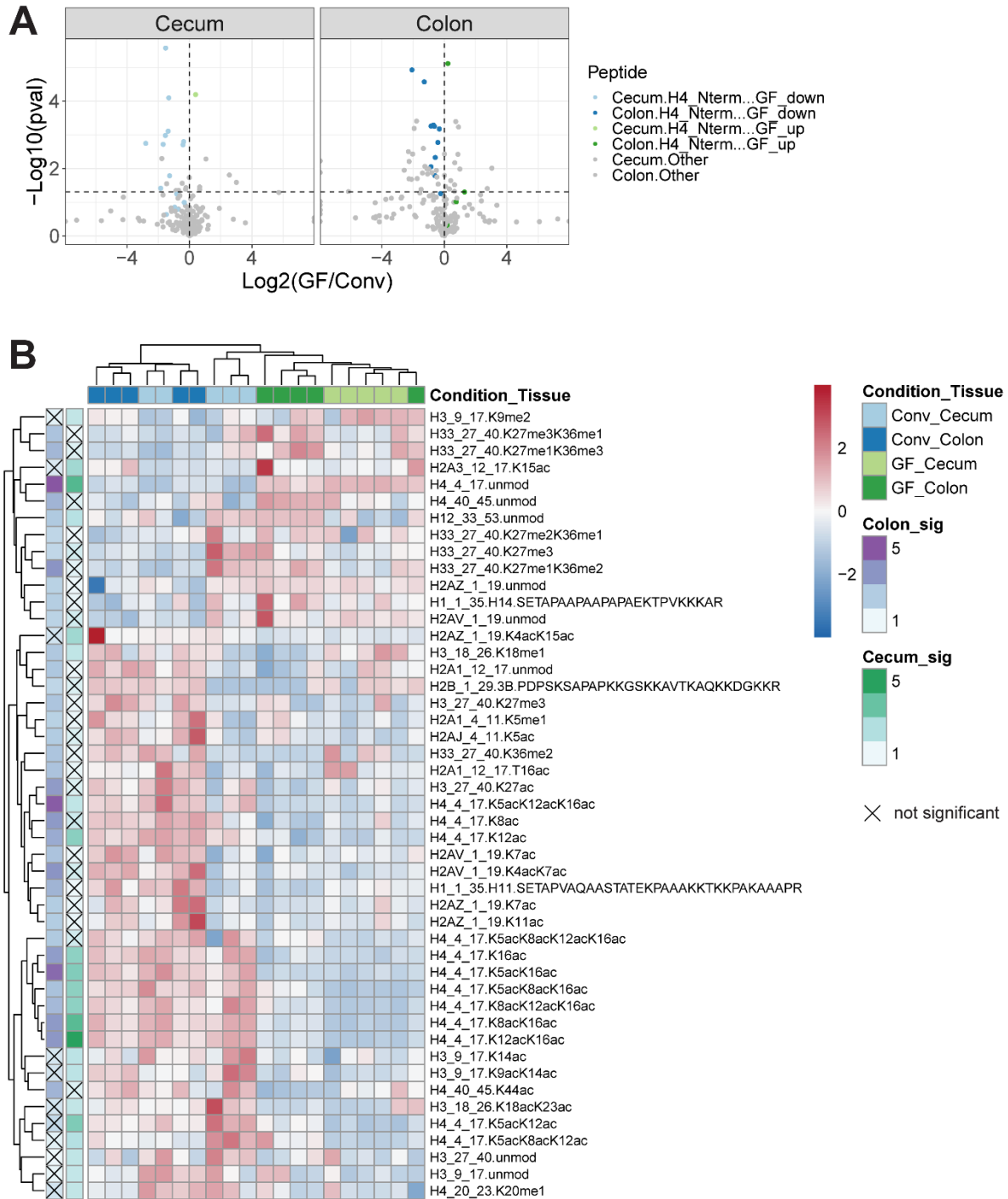


**Cell Reports, Volume 41**

**Supplemental information**

**Stable isotope tracing *in vivo* reveals  
a metabolic bridge linking the microbiota  
to host histone acetylation**

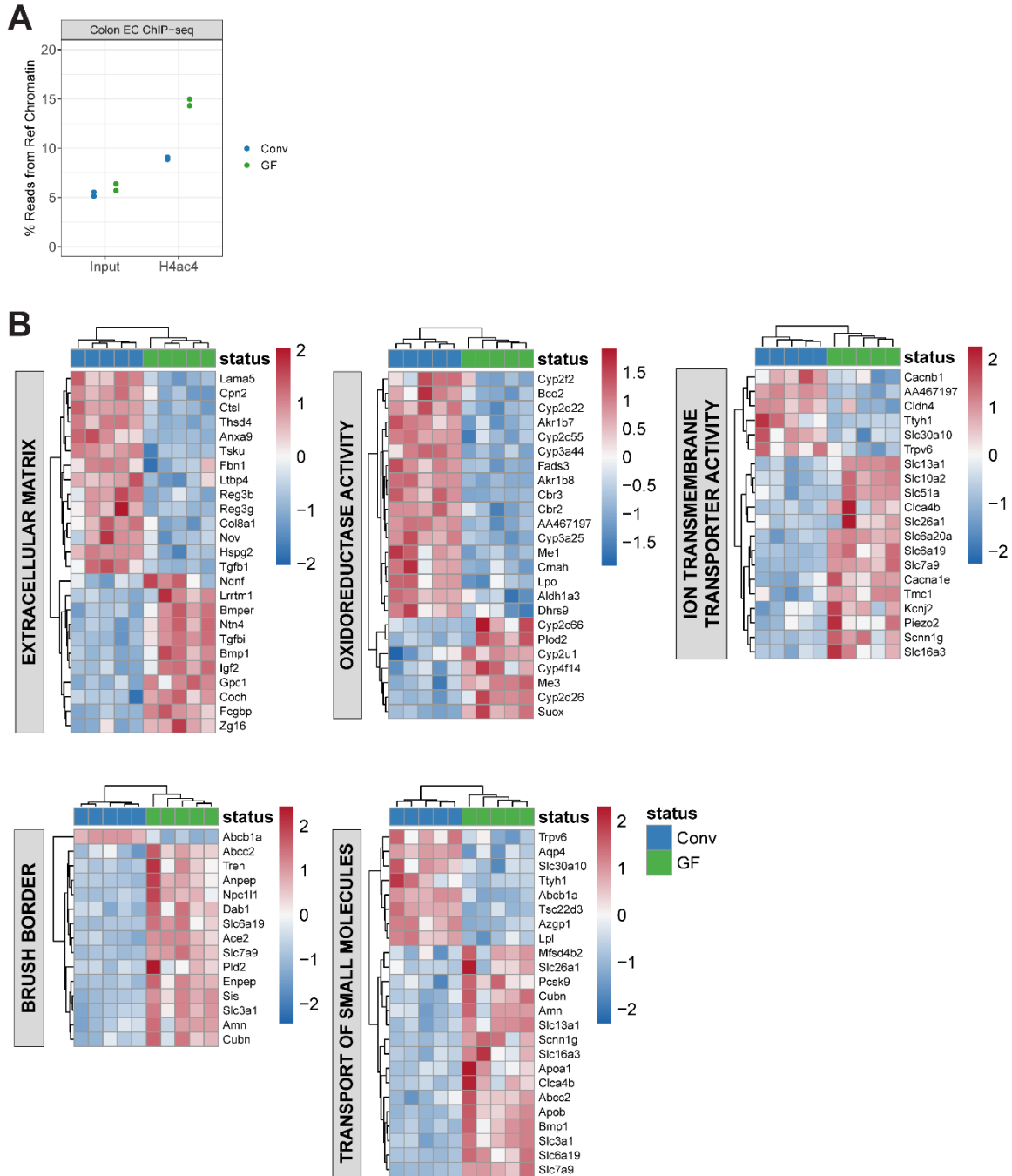
**Peder J. Lund, Leah A. Gates, Marylene Leboeuf, Sarah A. Smith, Lillian Chau, Mariana Lopes, Elliot S. Friedman, Yedidya Saiman, Min Soo Kim, Clarissa A. Shoffler, Christopher Petucci, C. David Allis, Gary D. Wu, and Benjamin A. Garcia**



**Supplemental Figure 1. Global profiling of histone modification patterns in the cecum and colon of germ-free versus conventional mice. Related to Figure 1B.**

A) Volcano plot of fold-change versus statistical significance for uniquely modified histone peptides across each tissue (cecum: 198, colon: 199). Peptides from the N-terminal tail of histone H4 (4-17 aa) are shown in green and blue while all other peptides are shown in gray. A horizontal dashed line is shown at  $-\log_{10}(0.05)$ . An unpaired, two-tailed Welch's t-test was used for statistical significance ( $n = 5$ ).

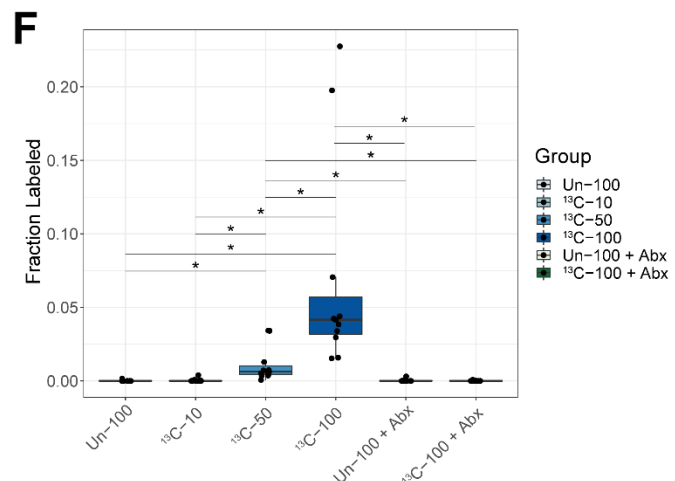
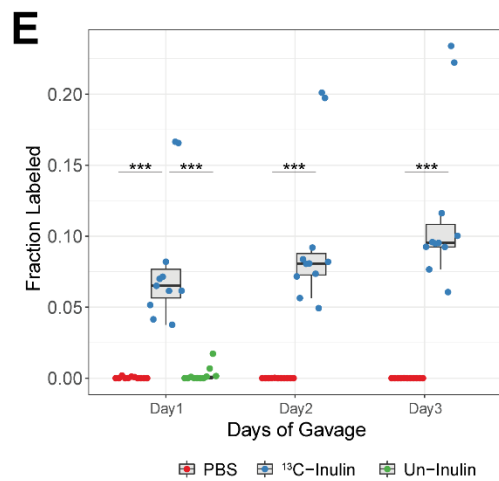
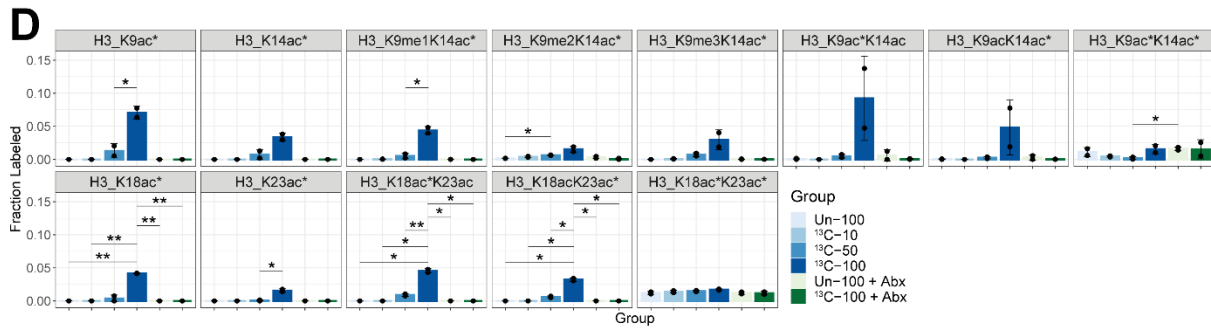
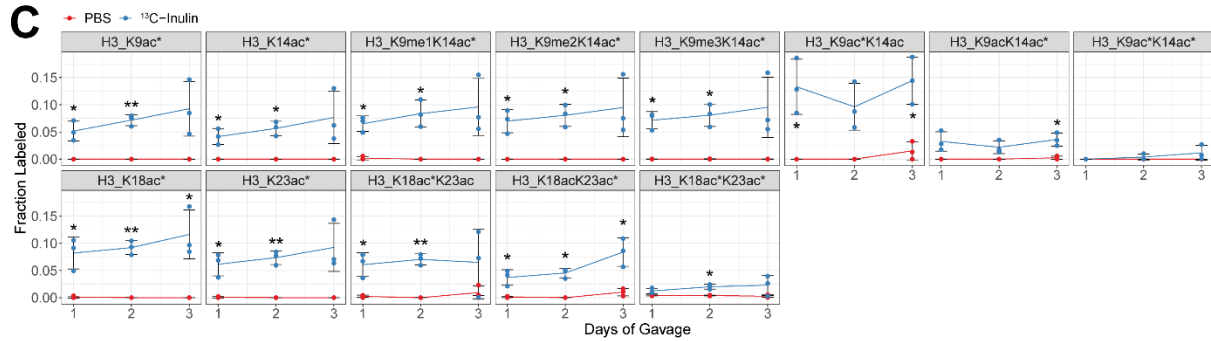
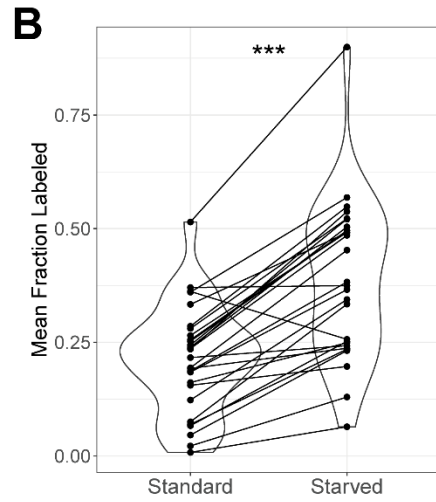
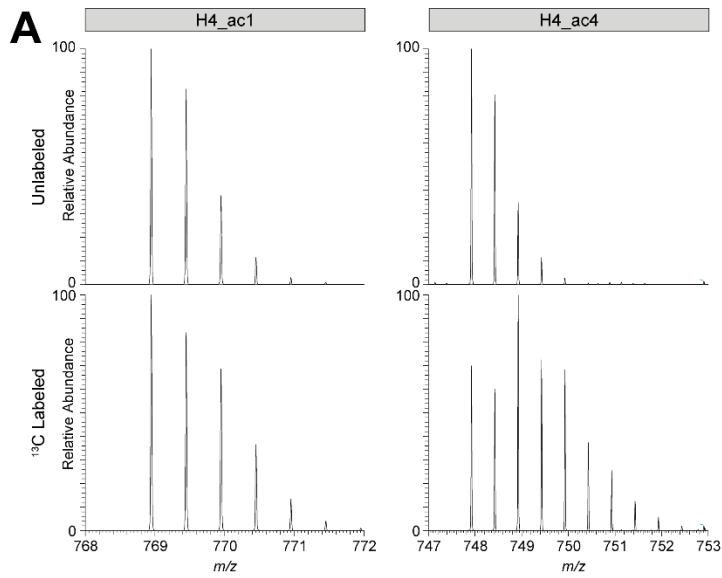
B) Heatmap of histone peptides with significant changes ( $p < 0.05$  by unpaired, two-tailed t-test) in their relative abundance in the ceca or colons of GF versus Conv mice. Each peptide is annotated with its parent histone protein, its starting and ending amino acid positions, and its post-translational modifications (unmod: unmodified, ac: acetyl, me1: mono-methyl, me2: di-methyl, me3: tri-methyl). The  $-\log_{10}(pval)$  in each tissue (Colon\_sig, Cecum\_sig) is represented in boxes on the left side.



**Supplemental Figure 2. Analysis of H4ac4 ChIP-seq and RNA-seq in colonic epithelial cells from conventional versus germ-free mice. Related to Figure 1C, 1D.**

A) The percent of uniquely mapping reads aligning to the *Drosophila* exogenous reference genome is plotted for input and H4ac4 ChIP samples from Conv and GF mice.

B) Heatmaps of differentially expressed genes belonging to significantly enriched pathways (GO or Reactome) in colonic epithelial cells from Conv versus GF mice.



**Supplemental Figure 3. Detection of isotope incorporation into histone acetyl groups after treatment with <sup>13</sup>C-butyrate in cell culture and <sup>13</sup>C-inulin in mice. Related to Figure 2.**

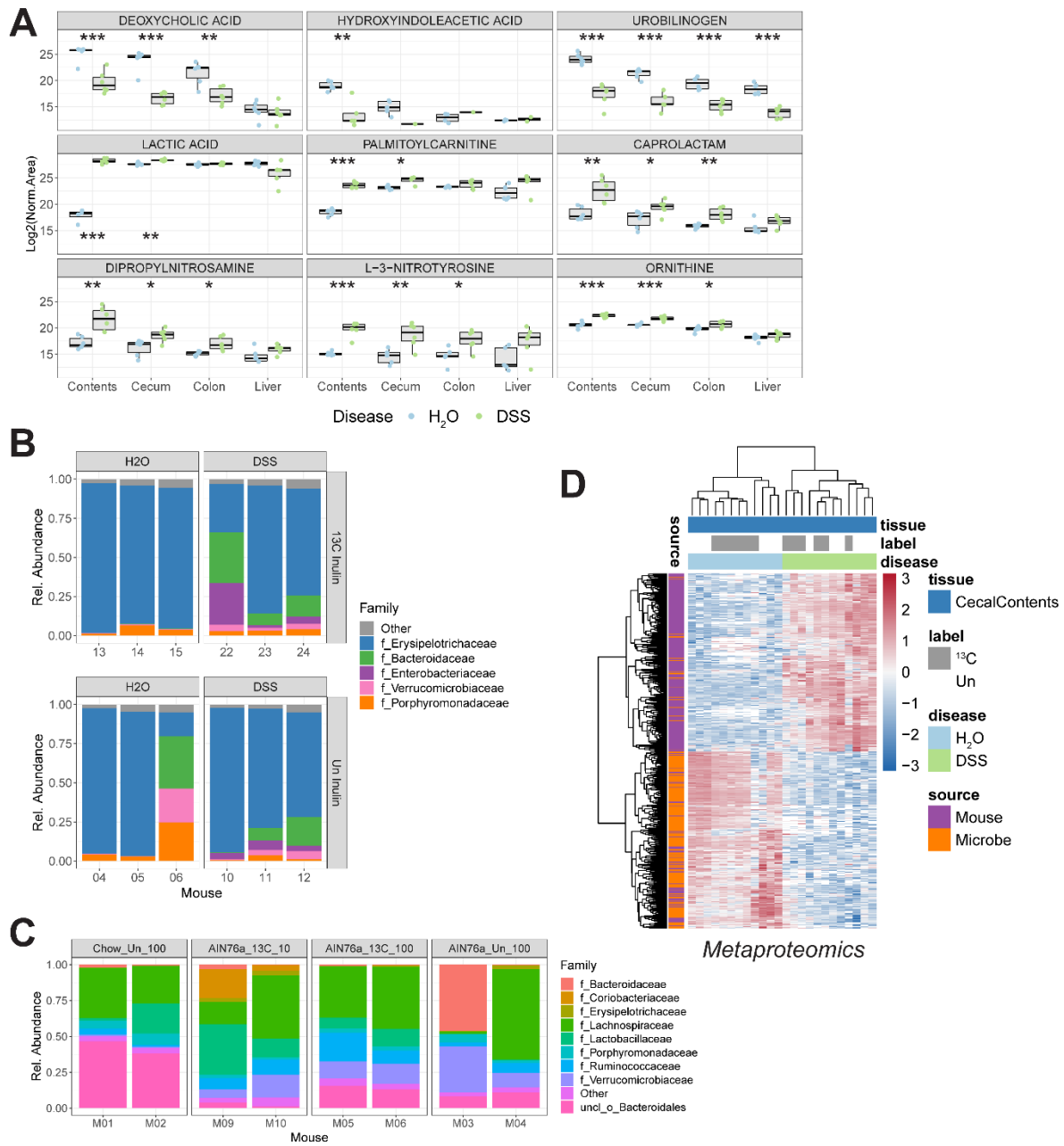
A) Mass spectra for precursor peptide ions corresponding to the histone H4 tail peptide (<sup>4</sup>GKGGKGLGKGGAKR<sup>17</sup>) carrying one (ac1) or four (ac4) acetyl groups after incubation of Caco2 cells with 1 mM unlabeled or U-<sup>13</sup>C-labeled butyrate for 24 hrs.

B) Caco2 cells were incubated with 1 mM U-<sup>13</sup>C-butyrate under standard or starved (1% dialyzed FBS – glucose – pyruvate) conditions for 24 hrs. Isotope incorporation into 28 acetylated peptides from histones H3 and H4 is shown with lines connecting the same peptides across conditions. Each point represents the mean of 2 technical replicates. \*\*\* p = 2.75 x 10<sup>-9</sup> by two-tailed, paired t-test.

C) Isotope incorporation over time for 13 acetylated histone H3 peptides in colonic epithelial cells from mice receiving daily gavages of <sup>13</sup>C-inulin or PBS (mean ± sd, n = 3). The top row shows peptides encompassing H3K9ac and H3K14ac while the bottom row shows peptides encompassing H3K18ac and H3K23ac. \* p < 0.05, \*\* p < 0.01 by unpaired, two-tailed Welch's t-test.

D) Isotope incorporation for 13 acetylated histone H3 peptides in colonic epithelial cells from mice receiving two daily gavages of labeled (<sup>13</sup>C) or unlabeled (Un) inulin at various doses (10, 50, 100 mg) with or without antibiotic treatment (Abx). Mean ± sd, n = 2. \* p < 0.05, \*\* p < 0.01 by unpaired, two-tailed Welch's t-test.

E, F) Summary of isotope incorporation measurements for acetylated histone H3 and H4 peptides from <sup>13</sup>C-inulin experiments. Each point represents the mean fraction labeled of an acetylated peptide (11 peptides from n = 3 mice in E or 2 mice in F). Only mono-acetylated peptides from histones H3 and H4 with one labeled acetyl group are displayed, including H3K9ac\*, H3K14ac\*, H3K9me1K14ac\*, H3K9me2K14ac\*, H3K9me3K14ac\*, H3K18ac\*, H3K23ac\*, H4K5ac\*, H4K8ac\*, H4K12ac\*, and H4K16ac\*. \* p < 0.05, \*\* p < 0.01, \*\*\* p < 0.001 by two-tailed, paired t-test comparing mean labeling of a given peptide across two groups.



**Supplemental Figure 4. Characterization of differences in metabolites, proteins, and microbiota composition between control and colitic mice. Related to Figure 3.**

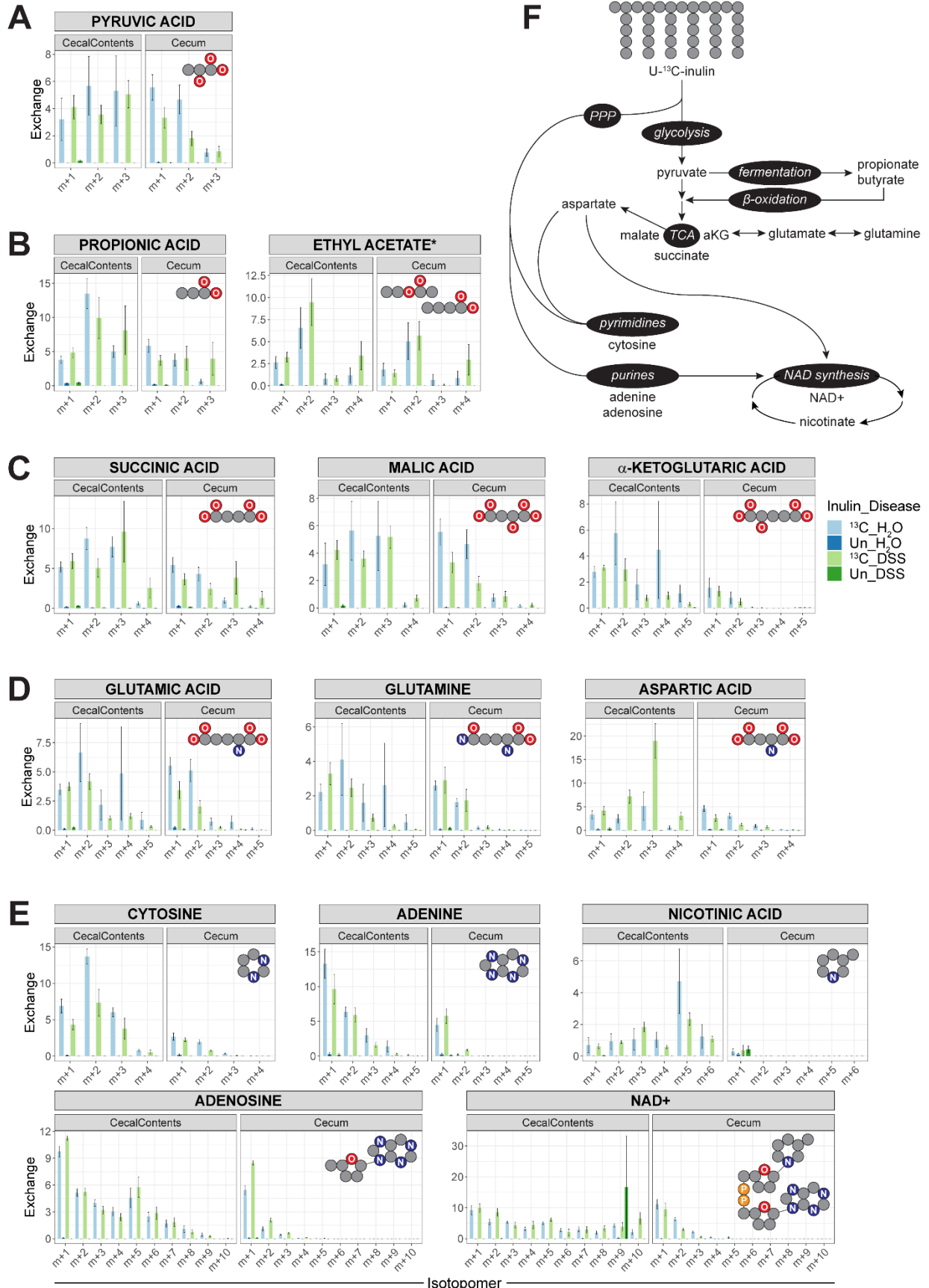
A) Normalized abundances of selected metabolites with significant differences. Both groups received Un inulin. Points indicate individual replicates ( $n = 6$ ) and box plots represent interquartile range with the median denoted by a heavy line. \*  $p < 0.05$ , \*\*  $p < 0.01$ , \*\*\*  $p < 0.001$  by unpaired, two-tailed t-test.

B) Relative abundances of different taxa at the family level based on 16S sequencing of cecal contents in control ( $H_2O$ ) and DSS mice after treatment with unlabeled (Un) or  $^{13}C$ -labeled ( $^{13}C$ ) inulin ( $n = 3$  mice per group).

C) Relative abundances of different taxa at the family level (except one group with classification to only the Bacteroidales order) based on 16S sequencing of cecal contents from selected groups from the experiment presented in Fig. 2E (n = 2 mice per group). Mice received either normal chow diet or the AIN76a diet and two gavages each of 10 or 100 mg of labeled ( $^{13}\text{C}$ ) or unlabeled (Un) inulin.

D) Heatmap of murine and microbial proteins showing differential abundance in the cecal contents of DSS mice by mass spectrometry (586 features,  $q < 0.01$ ). Missing values are displayed in white.

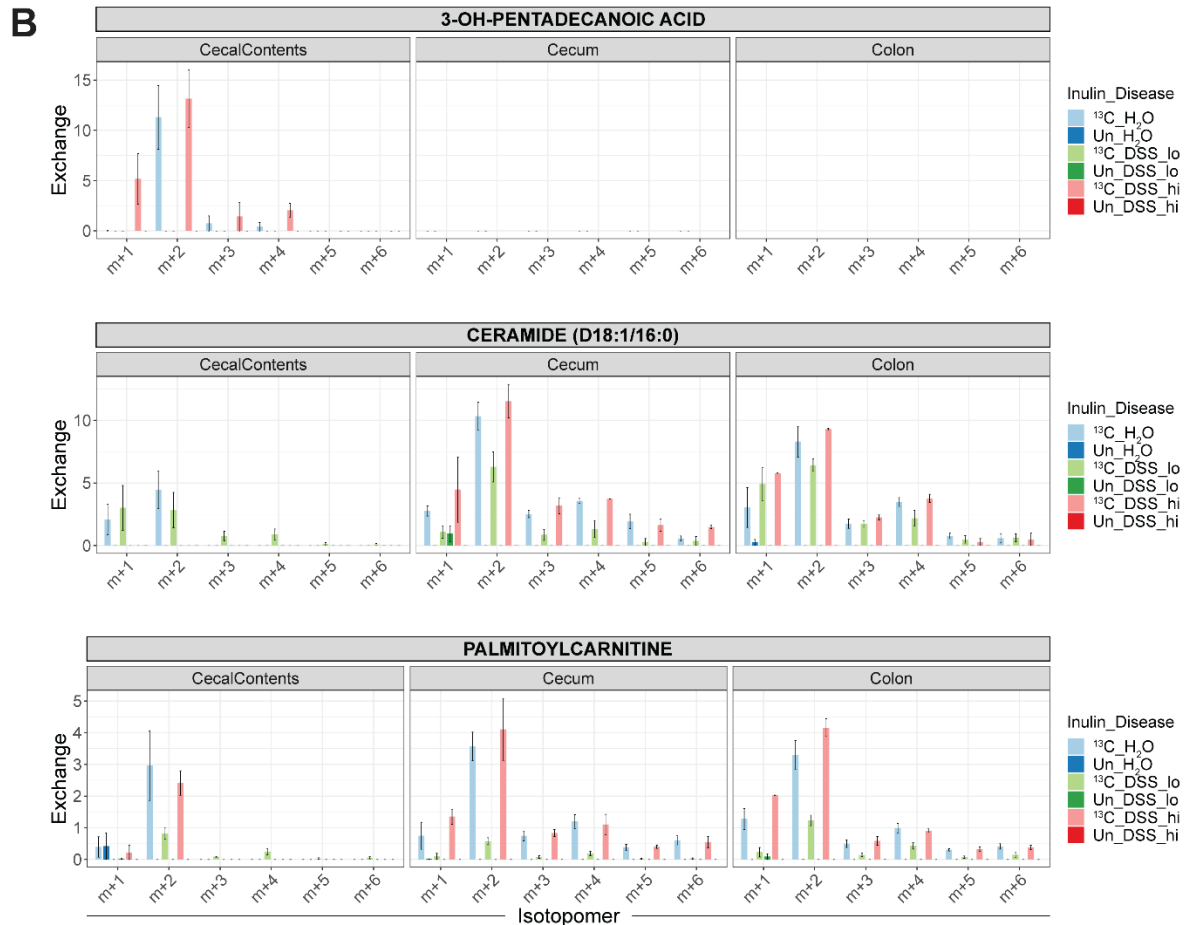
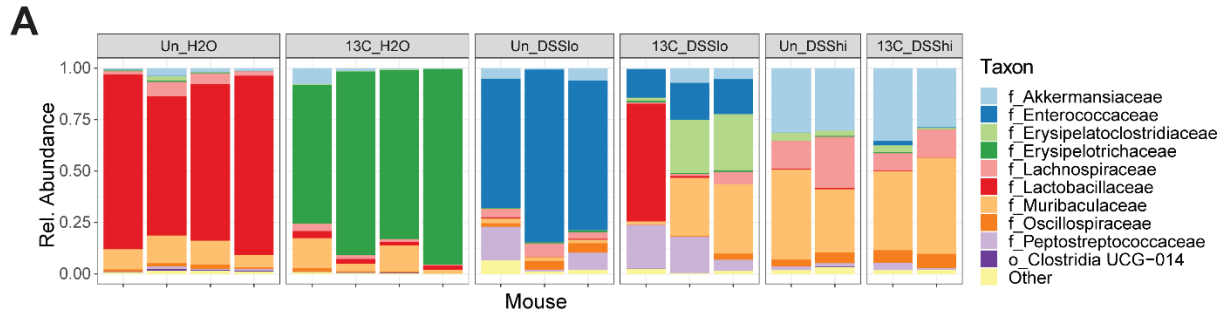




**Supplemental Figure 5. Contribution of dietary fiber to central carbon metabolism, nucleotide metabolism, NAD metabolism, and amino acid metabolism. Related to Figures 4 and 5.**

A-E) Isotopomer distributions for selected metabolites in the cecal contents and cecum from various pathways, including products related to glycolysis (A, pyruvate), fermentation (B, propionate and butyrate/ethyl acetate), TCA cycle (C, succinate, malate, alpha-ketoglutarate), amino acid synthesis (D, glutamate, glutamine, aspartate), and nucleotide and NAD synthesis (E, cytosine, adenine, nicotinate, adenosine, NAD<sup>+</sup>). In all cases, the m+0 peak is omitted for clarity. For NAD<sup>+</sup>, isotopomer peaks past m+10 are also omitted. Insets display simplified representations of carbon skeletons. \*Due to identical precursor masses, butyrate may have been erroneously identified ethyl acetate. Mean  $\pm$  sem, n = 6.

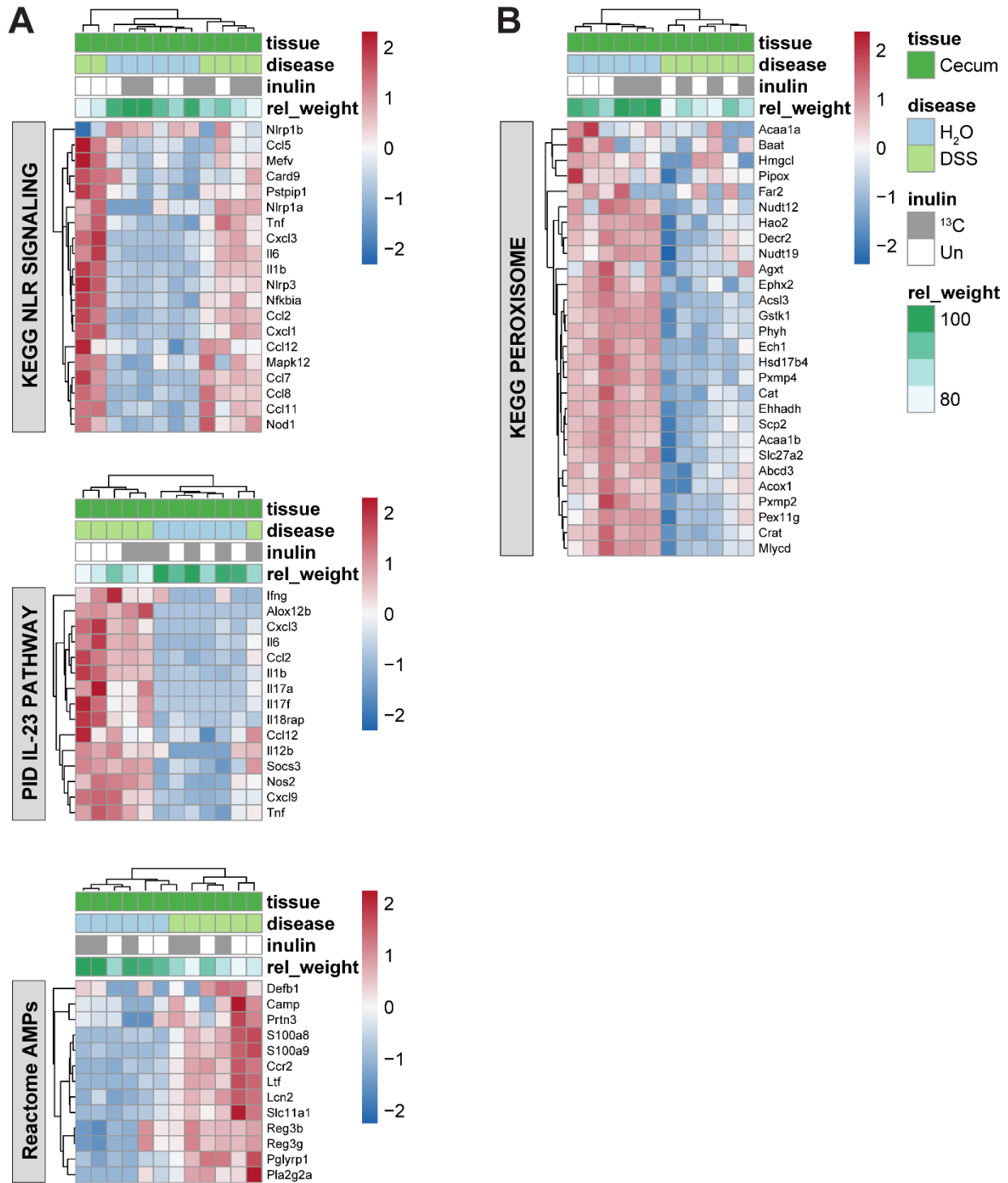
F) Schematic of putative routes of inulin metabolism. PPP: pentose phosphate pathway. TCA: tricarboxylic acid cycle.



**Supplemental Figure 6. Isotopic labeling of metabolites under different DSS treatments with different microbiota community compositions. Related to Figure 5.**

A) Microbiota community composition based on 16S sequencing of cecal contents. Mice were treated with labeled ( $^{13}\text{C}$ ) or unlabeled (Un) inulin and either normal drinking water ( $\text{H}_2\text{O}$ ) or drinking water with low (DSSlo, 36-50 kDa) or high molecular weight DSS (DSShi, 500 kDa). Each bar represents a different mouse ( $n = 2-4$  per group). Microbial taxa are displayed in different colors for families exceeding 5% mean relative abundance in an experimental group. Clostridia UCG-014 was only classified to the order level.

B) Isotopomer distributions for a long-chain fatty acid, a membrane lipid, and an acylcarnitine in the cecal contents, cecum, or colon of the same mice from A. Only the m+1 through m+6 isotopomers are shown for clarity. Mean  $\pm$  sem, n = 2-4 per group.



**Supplemental Figure 7. Transcriptional signatures present in the cecal tissue of control and colitic mice. Related to Figure 6.**

A, B) Heatmaps of GSEA core enrichment genes related to pathways upregulated (A) or downregulated (B) in DSS cecal tissue.